GEOLOGICA CARPATHICA, 2025, 76, 5, 337–351 https://doi.org/10.31577/GeolCarp.2025.19

Paleogeographic origin of the Cretaceous sandstones in the Apuseni and South Carpathian orogen, Romania: Implications from $^{40}Ar/^{39}Ar$ dating of detrital white mica

MARIA WIESINGER[1], FRANZ NEUBAUER[1,✉] and MANFRED BERNROIDER[1]

[1]Department of Environment and Biodiversity, Geology Division, Paris-Lodron-University of Salzburg, Hellbrunner Strasse 34, A-5020 Salzburg, Austria

(Manuscript received July 13, 2025; accepted in revised form November 1, 2025; Associate Editor: Igor Broska)

Abstract: Detrital white mica from two distinct Cretaceous stratigraphic levels and tectonic settings within the Apuseni Mountains (Mts.) and northernmost South Carpathians was dated using the single-grain $^{40}Ar/^{39}Ar$ technique in order to monitor the geodynamic evolution of this peculiar segment of the Cretaceous-aged Carpathian orogen. $^{40}Ar/^{39}Ar$ mica ages of a Lower Cretaceous synorogenic flysch succession in the Apuseni Mts. indicate the preservation of Early Variscan and Late Variscan orogenic metamorphic crust in the source region. By contrast, only a low percentage of Variscan micas have been detected in the post-orogenic Late Cretaceous Gosau-type Vlădeasa collapse basin of the Northern Apuseni Mts., which postdates the emplacement of the Mureş ophiolite belt and the Early to early Late Cretaceous formation of the low-grade metamorphic orogenic wedge. There, the studied micas are dominantly of early Late Cretaceous age and argue for the erosion of a medium-grade early Alpine metamorphic unit, which is not exposed in the surroundings of the present-day Apuseni Mts. Consequently, the Apuseni Mts. must have been either disrupted from such a source area and shifted along major strike-slip faults to the present position, or the source is now hidden. In contrast, the Late Cretaceous Gosau-type Rusca Montană basin of the South Carpathians comprises dominantly Variscan and a few Triassic detrital mica grains, consistent with Variscan and subordinate Triassic ages of the underlying and surrounding basement exposed in the Supra-Getic/Getic nappes.

Keywords: detrital white mica, exhumation, orogenic wedge, provenance, collapse basin, crustal rejuvenation

Introduction

Provenance studies based on dating of detrital minerals allow the determination of the minerals' source, especially when the hinterland is distinct in type and age of crystalline, metamorphic and plutonic, basement rocks. At present, the U–Pb zircon system is a widely used chronometer (e.g., Ducea et al. 2018), often in conjunction with further methods like the apatite and zircon (U–Th)/He chronometers (Obbágy et al. 2021), whereas the study of detrital white mica is subordinate although it yields rather information of the tectonothermal evolution than protolith ages (Hodges et al. 2005; Gemignani et al. 2017; Neubauer et al. 2025). $^{40}Ar/^{39}Ar$ white mica studies also reveal ancient tectonic processes in the source region as well as its tectonothermal history when insufficient data are known from the respective hinterland (e.g., Najman et al. 1997; von Eynatten et al. 1996; Hodges et al. 2005; Vozárová et al. 2005; Gemignani et al. 2017; Neubauer et al. 2025). We applied this method to constrain the Cretaceous tectonic evolution of the Apuseni Mountains (Mts.) and northernmost South Carpathians in southeastern Europe (Fig. 1a), particularly to determine (1) the distribution of the Alpine metamorphic overprint recorded in post-orogenic collapse basins (Gosau basins according to the type locality in the Eastern Alps), which follow Early to early Late Cretaceous nappe stacking and associated metamorphism, (2) the source-sink relationships of the infill of Late Cretaceous basins, and (3) the existence and distribution of Early Alpine (Cretaceous), Variscan vs. pre-Variscan tectonothermal overprint in the source regions.

Geological setting

The Northern Apuseni Mts. (Fig. 1b) constitute a nappe stack of basement-cover nappes (northern Apusenides), which comprise a Variscan, respectively pre-Variscan metamorphic basement and an Upper Carboniferous to basal Upper Cretaceous cover (Săndulescu 1984; Dallmeyer et al. 1999; Pană et al. 2002; Schmid et al. 2008; Merten et al. 2011; Kounov & Schmid 2012; Reiser et al. 2017). In the South Apuseni Mts., these nappes are overthrusted by the Jurassic Mureş ophiolite (Gallhofer et al. 2015) and synorogenic turbidite successions of Late Jurassic–Early Cretaceous age. The basement-cover nappes of the North Apuseni Mts. are overlain by Campanian–Maastrichtian Gosau-type sediments (Schuller 2004; Schuller et al. 2009 and references therein). Similar units are also known from the South Apuseni Mts., where these are incorporated in

✉ corresponding author: Franz Neubauer
franz.neubauer@plus.ac.at

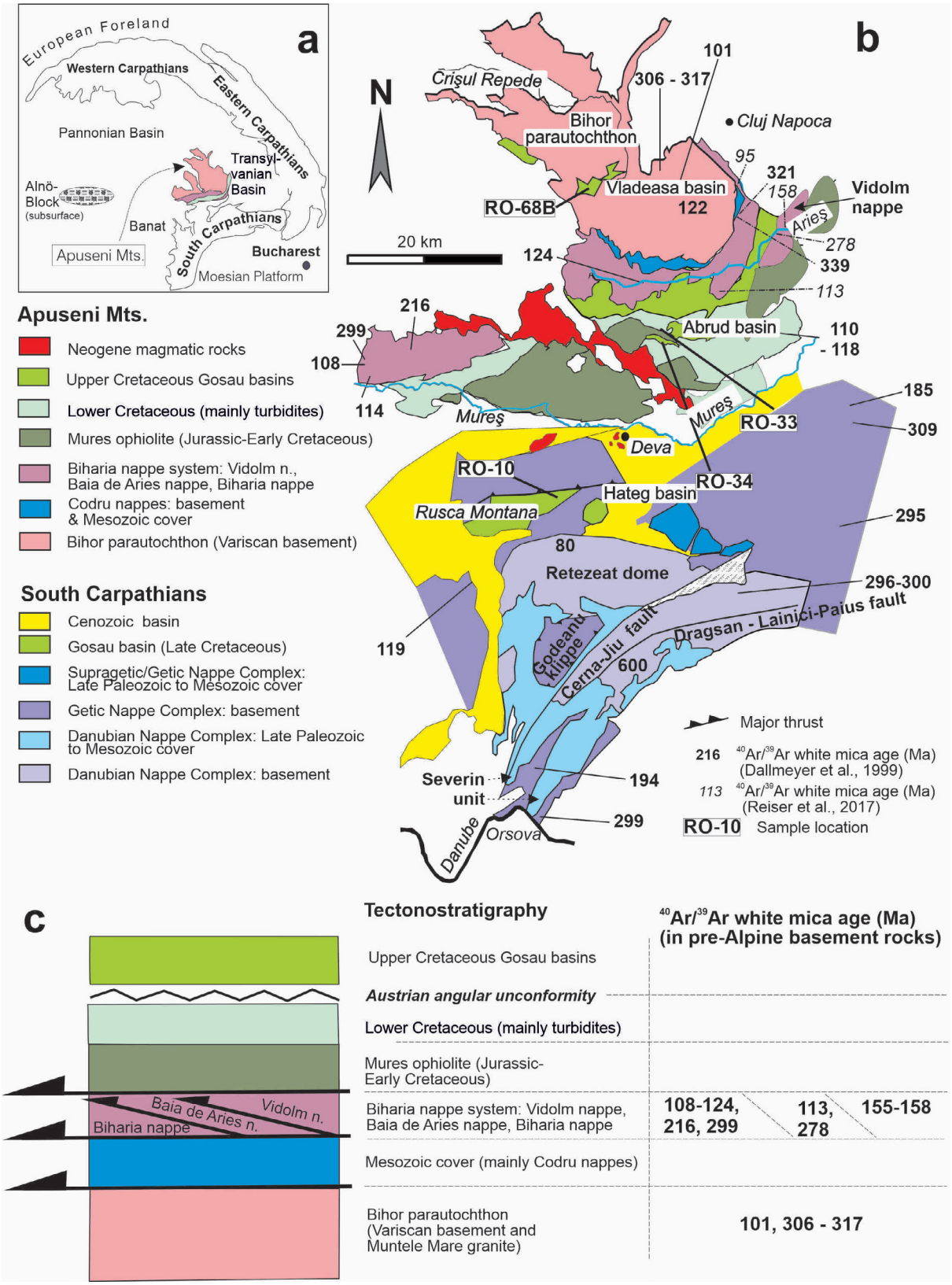

Fig. 1. a — Geological sketch map of the Alpine–Carpathian–Dinaride–Balkan orogenic belt with the location of the Apuseni Mts. **b** — Map of the Apuseni Mts. and South Carpathians and locations of dated samples. Previous $^{40}Ar/^{39}Ar$ white mica ages from pre-Upper Cretaceous basement rocks are shown. For sources, see Dallmeyer et al. (1998a, 1999), Iancu et al. (2005), Reiser et al. (2017) and further references as cited in the text. Map modified after Schuller (2004). **c** — Tectonostratigraphy of the Apuseni Mts. and distribution of $^{40}Ar/^{39}Ar$ white mica ages in basement rocks.

a post-Gosau nappe stack. Gosau basins are collapse-type, post-orogenic basins, which formed after the Cretaceous orogeny in the Austroalpine and correlative units of the Carpathians (Neubauer 2002; Schuller et al. 2009 and references therein; Bojar et al. 2010; Vornicu et al. 2023). The Late Cretaceous Gosau basins are named after the type locality in the Eastern Alps, are filled with terrestrial and subsequent marine clastic successions and are post-orogenic in respect to the Early to early Late Cretaceous Austrian orogenic phase (Wagreich & Faupl 1994 and references therein).

The basement units of the nappe stack exposed in the North Apuseni Mts. comprise a Variscan metamorphic basement with late Cambrian and Ordovician protoliths in the basement of Biharia, Baia de Arieş and Vidolm nappes (Fig. 1c) and mainly late Carboniferous to Permian granitoids in the Bihor parautochthon unit (Balintoni et al. 2010) (Fig. 1b), and some small, mainly amphibolite-rich basement and Mesozoic cover, units exposed in the Codru nappe system. The $^{40}Ar/^{39}Ar$ white mica ages of all these units cluster at (1) ca. 300 to 320 Ma and (2) ca. 404 Ma (Dallmeyer et al. 1996, 1999), whereas age of 95 Ma was found in the easternmost Bihor parautochthon and 278 Ma in the Vidolm nappe in its hanging-wall (Reiser et al. 2017) (Fig. 1b, c). These units and associated cover rocks are variably overprinted by low-grade Alpine metamorphism, which formed only fine-grained white mica (sericite with grain sizes at ca. 80–100 μm) with ages ranging from 101 to 124 Ma (Dallmeyer et al. 1996, 1999), respectively at 113 Ma (Reiser et al. 2017). Only the basement of the Baia de Arieş unit (Fig. 1) comprises well recrystallized medium-grade metamorphic rocks with a $^{40}Ar/^{39}Ar$ amphibole age of ca. 155 Ma (Dallmeyer et al. 1996, 1999), whereas basement amphibolites of the Codru nappe east of the Bihor parautochhon yielded amphibole ages of 366, 372 and 404 Ma (Dallmeyer et al. 1999). This age is interpreted to record Alpine metamorphism. A similar $^{40}Ar/^{39}Ar$ white mica age of 157.9±0.5 Ma was reported by Reiser et al. (2017). Zircon and apatite fission track ages of the northern and southeastern Apuseni Mts. demonstrate a Late Cretaceous age of cooling of large portions of Apuseni basement (Merten et al. 2011; Kounov & Schmid 2012; Reiser et al. 2017). Lelkes-Felvári et al. (2003) described a widespread amphibolite-grade metamorphic succession (Alnö block; Fig. 1a) with Late Cretaceous $^{40}Ar/^{39}Ar$ mica age of metamorphism from drill-holes in the basement of the Neogene Pannonian basin to the west of the Apuseni Mts. Recently, Kondor & Tóth (2025) demonstrated a two-stage metamorphism in the Alnö block reaching maximum ~9.5–10.5 kbar and ~670–720 °C during Variscan M1 and ~6.5–7.0 kbar and ~550–580 °C during Early Alpine (Cretaceous) M2 metamorphism.

The South Carpathians expose from footwall to hanging-wall (1) the Danubian nappe complex, a basement-cover complex with mainly Pan-African basement (Liégeois et al. 1996), (2) the Severin unit, an Upper Jurassic ophiolite-turbidite succession, which was sutured during the early Late Cretaceous, and (3) the Getic–Supragetic nappe complex with an exclusively Variscan metamorphic basement (Iancu et al. 2005). The Danubian nappe complex is exposed in the Danubian window and comprises a high-grade metamorphic basement with an $^{40}Ar/^{39}Ar$ white mica age of ca. 600 Ma and a few remnants of a Variscan basement (Dallmeyer et al. 1996, 1998a; Iancu et al. 2005). Basement rocks of Getic and Supragetic nappes are mainly affected by the Variscan eclogite metamorphism between 358 and 316 Ma (Medaris et al. 2003; Săbău & Massonne 2003) and show $^{40}Ar/^{39}Ar$ white mica ages between 315 and 280 Ma (Dallmeyer et al. 1996, 1998a). The Alpine metamorphic overprint in the South Carpathians is weak and only reaches upper greenschist facies´ conditions in small portions of the Danubian window (Iancu et al. 2005; Ciulavu et al. 2001). $^{40}Ar/^{39}Ar$ and K–Ar white mica ages of shear zones are either at ca. 200 Ma, interpreted to represent shear zone formation during the rifting period of the future Severin oceanic basin, or between 100 and 70 Ma due to shear zone formation during nappe stacking (Ratschbacher et al. 1993; Dallmeyer et al. 1998a). An older age (119 Ma) was found along the thrust contact between the Getic and Supragetic nappes in cover sediments (Dallmeyer et al. 1996). More recently, Neubauer & Bojar (2013) reported single-grain age populations of detrital white mica from the synorogenic Lower to lowermost Upper Cretaceous Sinaia Fm. flysch of the Danubian cover and Severin nappe. These ages include a Variscan population (288±4 to 329±3 Ma), which prove the Getic/Supragetic source with its dominating Variscan ages between 301 and 309 Ma (Dallmeyer et al. 1998a) of the infill of the Sinaia trench. Subordinately, Late Permian (255±10 to 263±8 Ma), Early Jurassic (183±3 and 185±4 Ma), Late Jurassic/Early Cretaceous (149±3 and 140±3 Ma) and a single Late Cretaceous age (98±4 Ma) were found in this study, too. The Late Permian to Early Cretaceous ages are interpreted to represent the exposure of likely retrogressive low-grade metamorphic ductile shear zones of various epochs or could represent "mixed", partly Variscan ages overprinted by low-grade (<375 °C) Early Alpine metamorphism.

Post-orogenic Gosau-type basins both in the Apuseni Mts. and South Carpathians formed due to extensional collapse of the over-thickened orogenic wedge during the Late Cretaceous (e.g., Willingshofer et al. 1999, 2001 and references therein; Schuller 2004; Schuller & Frisch 2006; Schuller et al. 2009). The basin fill comprises mainly clastic rocks with some intercalations of intermediate to acidic volcanic rocks, particularly in the Rusca Montană basin (e.g., Vornicu et al. 2023). In the adjacent, well studied Hateg basin, volcanics are subordinate. These volcanics are the surface expression of the so-called Banatite plutonic suites (Berza et al. 1998; Neubauer 2002; von Quadt et al. 2005; Vander Auwera et al. 2016; Gallhofer et al. 2017), which stretch from the Northern Apuseni Mts. to the western South Carpathians (Banat) and extend further through Serbia to Bulgaria. The depositional environment of the Hateg basin was recently described by van Itterbeek et al. (2004), Therrien (2005, 2006), Barzoi & Seclaman (2010), Bojar et al. (2010) and Melinte-Dobrinescu (2010). Willingshofer et al. (1999) suggested the main source of clastic material to be the hanging-wall unit, the Getic nappe complex, of the exhuming

Cretaceous-aged low-grade metamorphic Retezeat dome, which contains Danubian units. Consequently, exclusively Variscan detrital white mica could be expected as in the Getic basement exclusively Variscan white mica ages are recorded (Dallmeyer et al. 1998a). Berza (2004) demonstrated that the Danubian units were not exposed yet at the surface during pre-Maastrichtian times.

In the Apuseni Mts., a wildflysch of Late Aptian to Hauterivian age is considered to represent a synorogenic trench-type deposit, which formed during the emplacement of the tectonic nappes and build-up of an over-thickened orogenic wedge (Sandulescu 1984). Later, after a short period of surface erosion, the over-thickened orogenic wedge started to erode, and the Gosau-type basins formed as a sort of collapse basins in an overall extensional environment. The main source of the clastic material is considered to have been the hangingwall units above the Bihor parautochthon (e.g., Schuller & Frisch 2006). According to the $^{40}Ar/^{39}Ar$ white mica ages in bedrocks, mainly Variscan ages in coarse size fractions (>200 μm) and subordinate ages at ca. 154–160 Ma and between 95 and 120 Ma in very fine fractions (<160 μm) could be expected (Dallmeyer 1998a, 1999; Reiser et al. 2017).

Four sandstone samples (Fig. 1b) were selected for $^{40}Ar/^{39}Ar$ single-grain white mica analysis in this first-order study. Details of sample locations and stratigraphic setting are described in Appendix 1. Two samples (RO-33 and RO-34) are from the South Apuseni Mts. Sample RO-34 is from the wildflysch unit of Late Aptian to Hauterivian age (part of the Lower Cretaceous turbidites in Fig. 1b), sample RO-33 is from an overlying detrital Maastrichtian formation ("Sandy-Shaly Flysch": Bordea 1971; Bordea & Constantinescu 1975), which is part of the Abrud Basin (Fig. 1b). Schuller (2004) included this sequence in the Upper Cretaceous Gosau Group. Therefore, the results of these two samples should reflect the change from synorogenic trench fill to late- to post-orogenic molasse-type deposits. From these two samples, we used the grain size fraction 125–250 μm to register also possible Alpine mica grains with ages between 95 and 160 Ma. A smaller grain size is excluded for methodological reasons (low yield of radiogenic ^{40}Ar).

Sample RO-68B (grain size fraction: 250–355 μm) is from a Lower Maastrichtian level of the Gosau-type Vlădeasa basin of the North Apuseni Mts., a basin mostly filled with acidic volcanic flows. Sample RO-10 (grain size fraction: 125–250 μm) is from a Maastrichtian volcano-sedimentary formation in the Rusca Montană Gosau-type basin of the north-western South Carpathians.

$^{40}Ar/^{39}Ar$ age dating results

$^{40}Ar/^{39}Ar$ analytical techniques largely follow descriptions given in Handler et al. (2004) and Ilic et al. (2005) and are described in detail in Appendix 2. $^{40}Ar/^{39}Ar$ analytical results are presented in Tables 1 (stepwise heating of single grains) and 2 (single-grain total fusion). Results are graphically shown in Figs. 2 and 3. We selected a relatively small grain size (125–355 μm) to reveal the effects of the low-grade Alpine metamorphic overprint. Consequently, these grains are largely too small to perform systematic stepwise heating experiments. However, the results of a few successful stepwise heating experiments from one grain of sample RO-33 and two grains from sample RO-68B are shown in Fig. 2. White mica (125–250 μm) from sample RO-33 yielded an almost undisturbed Ar release pattern with only three steps. Together, these steps constitute a plateau-like integrated age of 269±15 Ma (Fig. 2; for a plateau, four steps are needed). The two high laser energy steps 2–3 show larger errors, mainly due to the small grain size and consequently low ^{39}Ar release.

White mica (250–355 μm) from single grain (grain a) of sample RO-68B/a yielded a plateau age of 163.5±1.4 Ma for steps 1–4 comprising 97.9 % of ^{39}Ar released. Steps 1–5 of grain b from the same sample (RO-68B/b) yielded a plateau age of 94±1 Ma comprising 97.4 % of ^{39}Ar released. The release pattern is slightly disturbed at the end due to the low amount of ^{39}Ar released.

Together, these three successful step-heating experiments display three different ages without any secondary overprint and represent, therefore, geologically meaningful ages. These ages (269±15, 163.5±1.4 and 94±1 Ma) can be interpreted either to represent formation ages of white mica crystallized under low-grade metamorphic conditions, or the ages of recrystallization or the ages of cooling through ca. 400–425 °C in the corresponding source regions (Harrison et al. 2009).

Results of single-grain total fusion experiments yield significant results (Fig. 3). Seventeen single white mica grains of sample RO-34, collected from the synorogenic flysch ("Shaly Flysch" of Hauterivian–Aptian age), resulted in two age clusters (Fig. 3a): (1) a major group of Variscan ages (295–342 Ma) and (2) a few Devonian ages ranging from 373 to 413 Ma.

Age clusters of sample RO-33, a molasse-type mica-rich sandstone ("Mica-Flysch") of Maastrichtian age of the South Apuseni Mts. show a significant change in composition compared to sample RO-34 and include: (Fig. 3b): (1) a major group of Variscan ages (320–352 Ma); (2) Permian ages ranging from 251 to 296 Ma; (3) a single Middle Triassic age (231 Ma); (4) several Alpine ages (140–150 Ma) as well (5) a Grenvillian age (1105±27 Ma). The Alpine age group likely reflects a metamorphic accretionary wedge. One grain represents a very old age of 1105±27 Ma Ma (Fig. 3c), but that age is not very reliable due to the large error of and the low amount of ^{39}Ar released.

Thirteen grains from sample 68B from the Maastrichtian Vlădeasa basin in the North Apuseni Mts. were measured. These display three age groups (Fig. 3d): two dominant Alpine age clusters ranging from (1) 65 to 98 Ma, respectively (2) from 118 to 130 Ma, and (3) two Permian ages of 263 and 273 Ma.

Thirteen single grains of sample RO-10 from the Maastrichtian Rusca Montană basin show three age clusters (Fig. 3e): (1) a Variscan group (318–340 Ma); (2) dominant Permian ages (252 and 279 Ma) and (3) one single grain with an apparent age of 208 Ma.

Table 1: $^{40}Ar/^{39}Ar$ analytical results of stepwise heating experiments on single grains.

	Sample RO-33, white mica (125–250), J-Value: 0.01534±0.00015									
step	**$^{36}Ar/^{39}Ar^{a}$**	**±**	**$^{37}Ar/^{39}Ar^{b}$**	**±**	**$^{40}Ar/^{39}Ar^{a}$**	**±**	**%$^{40}Ar^{c}$**	**%^{39}Ar**	**age [Ma]**	**±**
1	0.00000	0.00102	0.0000	0.0010	10.045	0.301	100.0	71.9	263.9	7.8
2	0.03397	0.00936	0.0000	0.0117	14.191	2.778	100.0	8.7	289.8	46.8
3	0.00000	0.00385	0.0000	0.0036	12.731	1.141	100.0	19.4	275.9	25.4
Steps 1–3								100.0	269.0	15.0
	Sample RO-68B/b, white mica (250–355), J-Value: 0.01535±0.00015									
step	**$^{36}Ar/^{39}Ar^{a}$**	**±**	**$^{37}Ar/^{39}Ar^{b}$**	**±**	**$^{40}Ar/^{39}Ar^{a}$**	**±**	**%$^{40}Ar^{c}$**	**%^{39}Ar**	**age [Ma]**	**±**
1	0.00783	0.00183	0.0000	0.0012	9.030	0.542	74.4	4.4	176.5	13.7
2	0.00000	0.00014	0.0000	0.0001	6.116	0.042	100.0	46.8	161.4	1.9
3	0.00000	0.00036	0.0000	0.0004	6.264	0.107	100.0	16.4	165.1	3.1
4	0.00000	0.00028	0.0000	0.0002	6.298	0.084	100.0	30.3	166.0	2.6
5	0.03214	0.00338	0.0000	0.0033	13.153	1.001	27.8	2.1	98.0	26.3
Steps 1–4								97.9	163.5	1.4
	Sample RO-68B/a, white mica (250–355), J-Value: 0.01535±0.00015									
step	**$^{36}Ar/^{39}Ar^{a}$**	**±**	**$^{37}Ar/^{39}Ar^{b}$**	**±**	**$^{40}Ar/^{39}Ar^{a}$**	**±**	**%$^{40}Ar^{c}$**	**%^{39}Ar**	**age [Ma]**	**±**
1	0.00000	0.00010	0.0000	0.0001	3.491	0.031	100.0	54.1	93.7	1.2
2	0.00000	0.00059	0.0000	0.0004	3.665	0.174	100.0	11.4	98.3	4.7
3	0.00000	0.00023	0.0354	0.0002	3.538	0.067	100.0	24.2	95.0	2.0
4	0.01032	0.00148	0.1041	0.0014	6.529	0.439	53.3	3.7	93.6	11.6
5	0.00000	0.00204	0.0221	0.0014	4.048	0.603	100.0	3.8	108.3	15.8
6	0.00890	0.00259	0.1246	0.0022	4.212	0.765	37.6	2.6	43.1	20.7
7	0.00000	0.02474	2.6356	0.0197	5.986	7.313	100.0	0.3	163.5	184.8
Steps 1–5								97.4	94.0	1.0

Errors of ratios, J-values and ages are at 1-sigma level.
a) measured
b) corrected for post-irradiation decay of ^{37}Ar
c) non-atmospheric ^{40}Ar

Microprobe results

As some high-pressure phengitic white mica grains were expected due to Cretaceous ages (like, e.g., in the correlative Austroalpine units of the Eastern Alps: Hoinkes et al. 1999), but also Variscan ones in the eclogite-bearing Getic basement of South Carpathians (Medaris et al. 2003; Săbău & Massonne 2003) we selected samples RO-10 and RO-68B from the Vlădeasa and Rusca Montană Gosau-type basins to determine the chemical composition of the white mica. The microprobe analytical technique is described in Appendix 3. The results are presented in Table 3 and Fig. 4.

As expected, both samples show a wide range of chemical compositions, from the pure muscovite endmember (low in Si per formula unit; Fig. 4) to several clusters with three distinct phengite compositions of sample RO-68A including a cluster of celadonite-rich phengite. In contrast sample RO-10 shows a continuity of muscovite endmember to phengite with a "medium" celadonite content (Fig. 4). A closer inspection of both samples reveals intergrown muscovite and phengite (Fig. 5) indicating that these micas coexisted during growth.

Discussion

The new data allow the discussion of important constraints of the paleogeographic evolution of the Cretaceous-aged Apuseni–South Carpathian orogen during the deposition of the two critical stratigraphic levels under consideration: (1) the synorogenic Hauterivian to Late Aptian flysch stage, and (2) the post-orogenic collapse-type stage of the Gosau basins of Late Cretaceous age (mainly "Senonian", respectively Maastrichtian). For discussion, the $^{40}Ar/^{39}Ar$ bedrock and detrital ages from the Apuseni Mts. are shown in Fig. 6.

The new data from the Lower and Upper Cretaceous sandstones of the Apuseni-South Carpathian orogen demonstrate the importance of the dominating Variscan orogeny in the source regions (Fig. 3f). This is in agreement with a similar study of detrital white mica in Jurassic–Lower Cretaceous graywackes related to the ophiolites of the Dinarides (Ilic et al. 2005), where classical Variscan detrital white mica ages (300–350 Ma) dominate. In sample RO-34, a few grains with older ages ranging from 378–413 Ma were detected. Detrital white mica grains of this age group are commonly found to have dominated the sedimentation in the Lower Carboniferous turbiditic foredeep in both the Bohemian massif (Schneider 2002) and some Paleozoic units in Eastern Alps (Handler et al. 1997; Mader et al. 2007; Neubauer et al. 2025) but not Mesozoic formations in the Alpine belt. However, the age group of 378–413 Ma is uncommon in basement rocks exposed in the South Carpathians and Apuseni Mts., which are dominated by Variscan and Permian white mica ages (Dallmeyer et al. 1998a, 1999). However, Dallmeyer et al. 2000; Culshaw et al. 2012) found this 378–413 Ma age group in some metamorphic basement units of the East Carpathians. Consequently, the synorogenic Lower Cretaceous-aged sandstone sample record

the denudation of deep levels of an early Variscan metamorphic accretionary wedge, which is obviously not exposed at present erosional levels in Apuseni Mts. but in the East Carpathians.

White mica grains originating from the classical Variscan age interval of ca. 300–330 Ma are important in the detrital mica record. Late Variscan, Permian to Early Triassic ages clustering around 243–300 Ma form a separate group similar

Table 2: $^{40}Ar/^{39}Ar$ analytical results of total fusion experiments on single grains.

	Sample RO-10, white mica (125–250), J-Value: 0.01535±0.00015									
grains	**$^{36}Ar/^{39}Ar^{a}$**	**±**	**$^{37}Ar/^{39}Ar^{b}$**	**±**	**$^{40}Ar/^{39}Ar^{a}$**	**±**	**%$^{40}Ar^{c}$**	**%$^{39}Ar^{d}$**	**age [Ma]**	**±**
1	0.00235	0.00074	0.0737	0.0008	14.242	0.220	95.1	8.6	340.6	5.9
2	0.00373	0.00065	0.0272	0.0007	14.503	0.193	92.4	8.6	337.1	5.4
3	0.00302	0.00045	0.0019	0.0005	8.904	0.133	90.0	13.6	208.9	3.8
4	0.00111	0.00053	0.0657	0.0005	12.923	0.157	97.5	11.1	318.6	4.7
5	0.00344	0.00089	0.1447	0.0008	13.837	0.265	92.6	6.5	324.0	6.8
6	0.00304	0.00044	0.0379	0.0004	12.575	0.131	92.9	14.3	297.1	4.1
7	0.00206	0.00027	0.0258	0.0003	11.283	0.080	94.6	22.0	273.4	3.2
8	0.00351	0.00039	0.0797	0.0003	11.059	0.116	90.6	15.3	258.0	3.7
9	0.00001	0.00082	0.0000	0.0009	11.261	0.245	100.0	16.1	287.2	6.4
10	0.00000	0.00051	0.0000	0.0006	9.784	0.150	100.0	28.1	252.1	4.3
11	0.00000	0.00064	0.0000	0.0007	11.246	0.189	100.0	21.7	286.9	5.2
12	0.00000	0.00080	0.0000	0.0006	10.093	0.237	100.0	16.9	259.5	6.2
13	0.00000	0.00076	0.0070	0.0009	11.248	0.225	100.0	17.1	287.0	5.9
	Sample RO-33, white mica (125–250), J-Value: 0.01534±0.00015									
grains	**$^{36}Ar/^{39}Ar^{a}$**	**±**	**$^{37}Ar/^{39}Ar^{b}$**	**±**	**$^{40}Ar/^{39}Ar^{a}$**	**±**	**%$^{40}Ar^{c}$**	**%$^{39}Ar^{d}$**	**age [Ma]**	**±**
1	0.00185	0.00019	0.0003	0.0002	13.239	0.055	95.9	20.6	320.6	3.2
2	0.00232	0.00021	0.0180	0.0002	5.980	0.062	88.5	17.0	140.5	2.1
3	0.00275	0.00037	0.0506	0.0003	13.476	0.111	94.0	10.8	320.0	3.9
4	0.00269	0.00051	0.0044	0.0005	14.327	0.152	94.5	7.3	339.9	4.7
5	0.00065	0.00032	0.0125	0.0003	14.261	0.094	98.6	11.3	352.2	3.9
6	0.00102	0.00031	0.0428	0.0003	11.128	0.091	97.3	12.2	276.9	3.4
7	0.00012	0.00045	0.0128	0.0003	13.377	0.132	99.7	11.2	335.6	4.3
8	0.00182	0.00045	0.0888	0.0004	9.484	0.132	94.3	9.8	231.8	3.9
9	0.00000	0.00040	0.0000	0.0004	10.685	0.120	100.0	11.0	273.5	3.8
10	0.00000	0.00063	0.0000	0.0006	5.686	0.185	100.0	8.4	150.5	4.9
11	0.00000	0.00553	0.0000	0.0037	55.144	1.686	100.0	1.0	1105.6	26.6
12	0.00000	0.00039	0.0000	0.0003	5.290	0.116	100.0	11.7	140.4	3.3
13	0.00835	0.00054	0.0015	0.0005	13.271	0.159	81.4	8.3	276.3	4.6
14	0.00012	0.00052	0.0000	0.0005	11.674	0.155	99.7	9.3	296.0	4.5
15	0.00000	0.00028	0.0000	0.0004	12.742	0.084	100.0	16.2	321.7	3.5
16	0.00000	0.00029	0.0000	0.0003	9.782	0.087	100.0	15.9	251.9	3.2
17	0.00047	0.00055	0.0000	0.0006	5.493	0.162	97.5	9.6	142.0	4.4
18	0.00094	0.00064	0.0000	0.0007	11.687	0.190	97.6	8.5	290.6	5.2
	Sample RO-34, white mica (125–250), J-Value: 0.01535±0.00015									
grains	**$^{36}Ar/^{39}Ar^{a}$**	**±**	**$^{37}Ar/^{39}Ar^{b}$**	**±**	**$^{40}Ar/^{39}Ar^{a}$**	**±**	**%$^{40}Ar^{c}$**	**%$^{39}Ar^{d}$**	**age [Ma]**	**±**
1	0.00034	0.00014	0.0111	0.0001	13.707	0.042	99.3	27.0	341.9	3.3
2	0.00280	0.00033	0.0777	0.0004	15.823	0.098	94.8	10.7	373.6	4.0
3	0.00211	0.00032	0.0798	0.0004	16.042	0.095	96.1	11.3	383.0	4.1
4	0.00533	0.00066	0.1231	0.0008	18.343	0.197	91.4	5.3	413.1	5.7
5	0.00031	0.00027	0.0165	0.0003	13.418	0.081	99.3	15.7	335.4	3.6
6	0.00039	0.00022	0.0277	0.0002	13.095	0.065	99.1	20.6	327.5	3.4
7	0.00073	0.00044	0.0782	0.0004	13.503	0.131	98.4	9.4	334.6	4.3
8	0.00199	0.00039	0.0000	0.0004	12.520	0.116	95.3	8.5	303.0	3.9
9	0.00000	0.00023	0.0000	0.0002	11.620	0.068	100.0	17.2	295.7	3.2
10	0.00000	0.00032	0.0000	0.0003	12.647	0.094	100.0	14.4	319.7	3.7
11	0.00000	0.00033	0.0000	0.0004	12.700	0.098	100.0	13.3	320.9	3.7
12	0.00000	0.00045	0.0000	0.0005	11.671	0.132	100.0	9.8	296.9	4.1
13	0.00000	0.00068	0.0000	0.0007	12.136	0.203	100.0	6.9	307.8	5.5
14	0.00482	0.00083	0.0626	0.0009	12.129	0.245	88.2	5.0	274.2	6.4
15	0.00145	0.00046	0.0609	0.0005	11.959	0.138	96.4	8.9	293.7	4.2
16	0.00136	0.00058	0.0000	0.0005	13.169	0.171	96.9	6.2	322.5	4.9
17	0.00000	0.00040	0.0000	0.0004	11.570	0.119	100.0	9.7	294.6	3.9

Table 2 (continued)

	Sample RO-68B, white mica (250–355), J-Value: 0.01535±0.00015									
grains	**$^{36}Ar/^{39}Ar^{a}$**	**±**	**$^{37}Ar/^{39}Ar^{b}$**	**±**	**$^{40}Ar/^{39}Ar^{a}$**	**±**	**$\%^{40}Ar^{c}$**	**$\%^{39}Ar^{d}$**	**age [Ma]**	**±**
1	0.00130	0.00009	0.0028	0.0001	3.703	0.027	89.6	16.8	89.2	1.1
2	0.00081	0.00005	0.0038	0.0001	3.416	0.016	93.0	26.8	85.5	0.9
3	0.00017	0.00009	0.0196	0.0001	10.737	0.027	99.5	15.7	273.5	2.6
4	0.00090	0.00023	0.0222	0.0002	3.629	0.067	92.6	6.4	90.4	2.0
5	0.00150	0.00020	0.0107	0.0001	3.607	0.058	87.7	7.7	85.1	1.8
6	0.00044	0.00005	0.0059	0.0000	4.560	0.015	97.1	26.6	118.2	1.2
7	0.00000	0.00009	0.0000	0.0001	3.467	0.027	100.0	22.8	93.1	1.2
8	0.00133	0.00017	0.0000	0.0002	3.381	0.051	88.4	12.4	80.4	1.6
9	0.00269	0.00055	0.0000	0.0003	3.972	0.162	80.0	6.1	85.5	4.4
10	0.00000	0.00031	0.0000	0.0001	10.283	0.092	100.0	17.8	263.9	3.3
11	0.00546	0.00027	0.0002	0.0004	4.028	0.081	59.9	8.9	65.2	2.3
12	0.00041	0.00027	0.0000	0.0003	3.778	0.078	96.8	16.1	98.1	2.3
13	0.00000	0.00018	0.0000	0.0003	4.887	0.054	100.0	15.8	130.0	1.9

Errors of ratios, J-values and ages are at 1-sigma level.
a) measured
b) corrected for post-irradiation decay of ^{37}Ar
c) non atmospheric ^{40}Ar
d) relative % ^{39}Ar of all single grains measured from the sample

as in Alps (von Eynatten et al. 1996; von Eynatten & Wijbrans 2003; Neubauer et al. 2025) and likely result from the combined effects of late Variscan orogenic collapse and ongoing Alpine, Permian rifting, a model that was already proposed by Dallmeyer et al. (1998a, b). A similar age group was recently reported from the East Carpathian basement (Culshaw et al. 2012).

The age cluster of 140–159 Ma found in the Maastrichtian molasse-type deposit overlying the Lower Cretaceous flysch is interesting and indicates that a Jurassic to earliest Cretaceous accretionary wedge-type metamorphic unit was possibly exposed in the source region. Similar ages from metamorphic units, the Baia de Arieş and Vidolm basement nappe (Figs. 1b, 6), were described by Dallmeyer et al. (1996, 1999) and Reiser et al. (2017). Therefore, the corresponding source might have been in the Baia de Arieş and Vidolm nappes above the Bihor parautochthon (Figs. 1b, 6), which were already eroded during the Maastrichtian. This corresponds with reported transport directions from the north as postulated by Schuller (2004) and Schuller et al. (2009). It is important to note that the 140–159 Ma age cluster indicates important tectonothermal processes during exhumation after the emplacement of the Mureş ophiolite.

In comparison, the age patterns of the two samples from the Late Cretaceous Gosau basins, sample RO-68B from the Vlădeasa basin in North Apuseni Mts.with three populations at 65 to 98 Ma, 118 to 130 Ma, 263 and 273 Ma and sample RO-10 from the Rusca Montană basin in South Carpathians with populations or grains at 318–340 Ma, 252 and 279 Ma, 208 Ma are more diverse. The Variscan and Permian ages from the Rusca Montana basin reflect the Variscan and Permian ages of the Supragetic and Getic basement in South Carpathians (Dallmeyer et al. 1998a).

In contrast, the Vlădeasa basin sample from the Apuseni Mts. suggest that amphibolite facies and higher greenschist facies grade metamorphic units of early Late Cretaceous age were already subject to erosion in the North Apuseni Mts. during the Late Cretaceous. Such metamorphic units are actually not widespread in Apuseni Mts., although the age group of predominantly 110–120 Ma is known in low-grade units

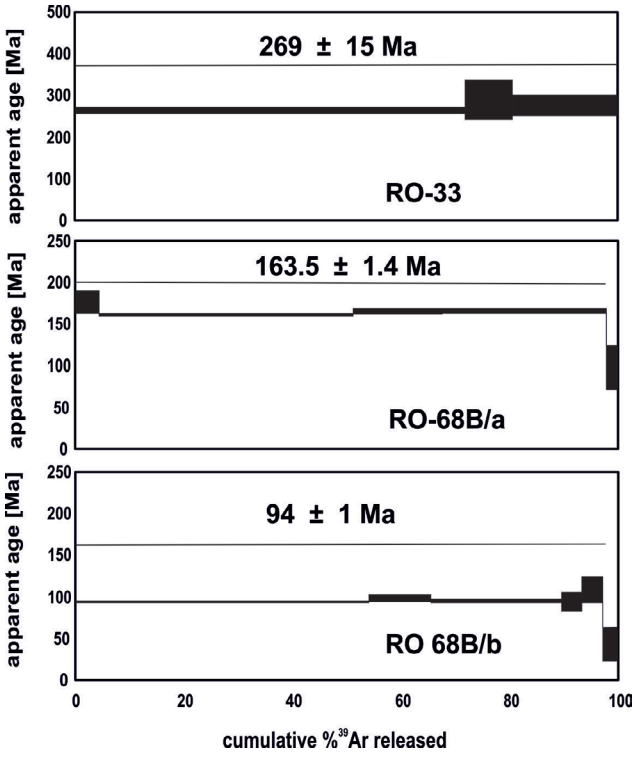

Fig. 2. $^{40}Ar/^{39}Ar$ apparent age patterns of stepwise heating experiments of single detrital white mica grains from samples RO-33 and RO-68B; both samples are from Apuseni Mts. Laser energy increases from left to right until fusion.

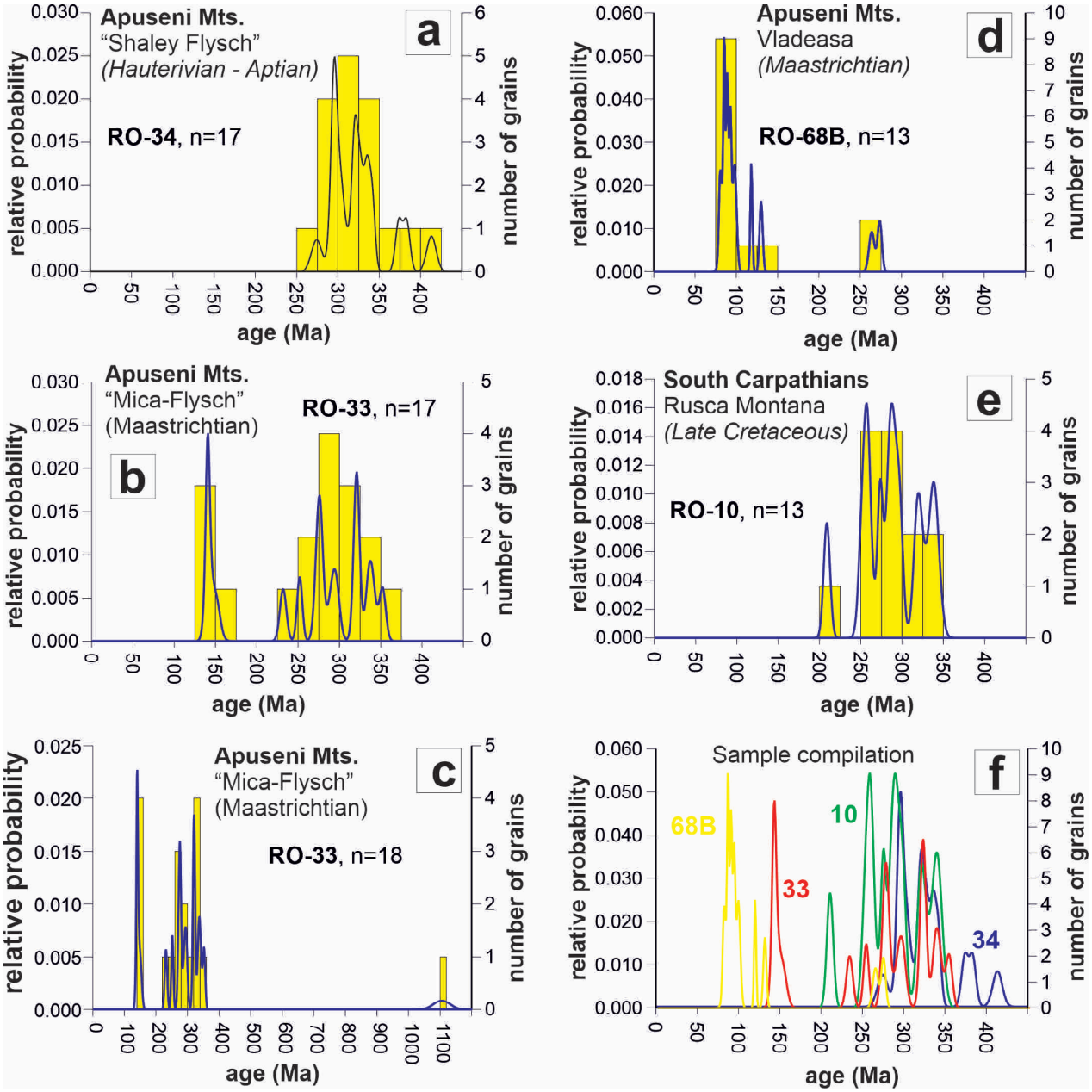

Fig. 3. Presentation of $^{40}Ar/^{39}Ar$ apparent ages of single detrital white mica grains. Combined age probability and histogram plots of all dated detrital white mica Ar–Ar ages using the AgeDisplay program of Sircombe (2004). **a** — Lower Cretaceous flysch unit. **b, c** — Maastrichtian "Mica flysch". **c** – The population also includes one white mica grain with an age of 1106 Ma. **d** — Vladeasa basin (Maastrichtian).**e** — Upper Cretaceous Gosau Group Rusca Montană, Late Cretaceous. **f** — This graph presents a data compilation of all white mica ages measured in this study.

(Dallmeyer et al. 1999; Reiser et al. 2017). However, only very fine-grained white micas (<100 μm) are recorded in these units (Dallmeyer et al. 1996, 1999) and can be excluded as a potential source. As mentioned before, zircon and apatite fission track ages of the northern and southeastern Apuseni Mts. demonstrate a Late Cretaceous age of cooling and therefore likely surface denudation of large portions of the Apuseni basement (Merten et al. 2011; Kounov & Schmid 2012; Reiser et al. 2017).

An interesting feature is the high proportion (>90 %) of new, Cretaceous-aged, micas in the Vlădeasa collapse-type basin of Maastrichtian age (sample RO-68B; Fig. 1b for location), although we used a relatively coarse grain size fraction (250–355 μm). Within the Apuseni basement, the only potential source is in the eastern hangingwall units of the Bihor parautochthon (Reiser et al. 2017), and in the eastern Baia de Aries nappe; Fig. 1b), which shows mostly older ages. This opens the question where a corresponding source region with

Table 3: Selected representative microprobe analyses (in weight percent) of white mica from samples RO-10 and RO-68B. Cations are in per formula units (pfu) on the basis of 22 oxygen atoms (on water-free basis). All iron is assumed to be Fe^{2+}. Abbreviations: Mu=muscovite, Ph=phengite.

	RO-10 Mu1	RO-10 Mu2	RO-10 Ph1	RO-10 Ph2	RO-10 Mu3	RO-10 Mu4	RO-68B Mu1	RO-68B Mu2	RO-68B Mu3	RO-68B Ph1	RO-68B Ph2	RO-68B Ph3	RO-68B Mu/Ph
SiO_2	47.82	46.94	49.06	48.95	44.41	44.96	45.13	43.49	44.81	48.06	48.96	50.29	48.44
TiO_2	0.42	0.41	0.34	0.45	0.46	0.43	0.30	0.31	0.31	0.31	0.33	0.22	0.25
Al_2O_3	33.70	32.47	27.40	27.75	35.13	34.44	34.72	34.09	34.09	24.46	24.28	25.06	26.51
MgO	0.99	1.38	2.90	2.77	0.79	1.00	0.58	0.55	0.62	3.06	3.30	3.16	2.95
CaO	0.01	0.00	0.00	0.01	0.01	0.03	0.02	0.05	0.03	0.16	0.09	0.07	0.07
MnO	0.00	0.00	0.00	0.00	0.00	0.00	0.00	0.01	0.00	0.00	0.04	0.04	0.01
FeO	1.02	1.37	2.38	2.19	1.00	1.15	0.82	1.29	0.85	3.61	3.51	3.53	2.51
Na_2O	0.63	0.51	0.16	0.12	0.78	0.82	1.06	0.39	1.19	0.28	0.20	0.25	0.22
K_2O	8.95	9.12	10.91	10.67	9.39	9.14	9.42	10.09	8.51	10.40	10.48	9.70	10.42
Total	93.53	92.20	93.14	92.92	91.97	91.97	92.05	90.27	90.41	90.32	91.18	92.35	91.38
Cations (O 22)													
Si	6.396	6.397	6.725	6.708	6.092	6.161	6.179	6.114	6.215	6.845	6.896	6.938	6.764
Ti	0.042	0.042	0.035	0.047	0.047	0.044	0.031	0.033	0.032	0.033	0.035	0.023	0.026
Al	5.311	5.216	4.427	4.482	5.680	5.562	5.602	5.648	5.573	4.105	4.031	4.080	4.363
Mg	0.198	0.280	0.592	0.566	0.161	0.204	0.118	0.116	0.128	0.650	0.694	0.650	0.613
Ca	0.001	0.000	0.000	0.001	0.001	0.004	0.003	0.007	0.005	0.024	0.013	0.010	0.010
Mn	0.000	0.000	0.000	0.000	0.000	0.000	0.000	0.001	0.000	0.000	0.004	0.005	0.001
Fe	0.114	0.156	0.273	0.251	0.115	0.132	0.093	0.152	0.098	0.429	0.413	0.407	0.293
Na	0.163	0.136	0.042	0.031	0.207	0.217	0.282	0.108	0.321	0.077	0.054	0.066	0.060
K	1.527	1.585	1.907	1.866	1.643	1.598	1.645	1.810	1.505	1.890	1.882	1.707	1.856
Total	13.75	13.81	14.00	13.95	13.95	13.92	13.95	13.99	13.88	14.05	14.02	13.88	13.98

age populations of 65 to 98 Ma and 263 and 273 Ma might occur. Possible sources for the 65 to 98 Ma population are the Alnö block in the pre-Neogene basement of the Pannonian basin (for location see Fig. 1a) as described by Lelkes-Felvári et al. (2003, 2005), and the East Carpathian nappe stack, from where Culshaw et al. (2012) and Dallmeyer et al. (2000) record similar $^{40}Ar/^{39}Ar$ ages (for locations, see Fig. 1a). The compositional white mica data of sample RO-10 show a white variation of compositions, which is in accordance with white mica compositional data from Alnö block (Lelkes-Felvári et al. 2005; Kondor & Tóth 2025) and support their interpretation of the derivation from the Alnö block or a similar unit in the west. Schuller & Frisch (2006) show that sedimentary transport directions of the Upper Gosau Subgroup are either from NW or S to SE, but no data exist for the Vladeasa basin. These authors propose also an E–W trend of the Gosau basin in the Southern Apuseni Mts. implying axial transport from W or E. The derivation from the Alnö block would imply axial transport from the west provided that no major displacement occurred after deposition.

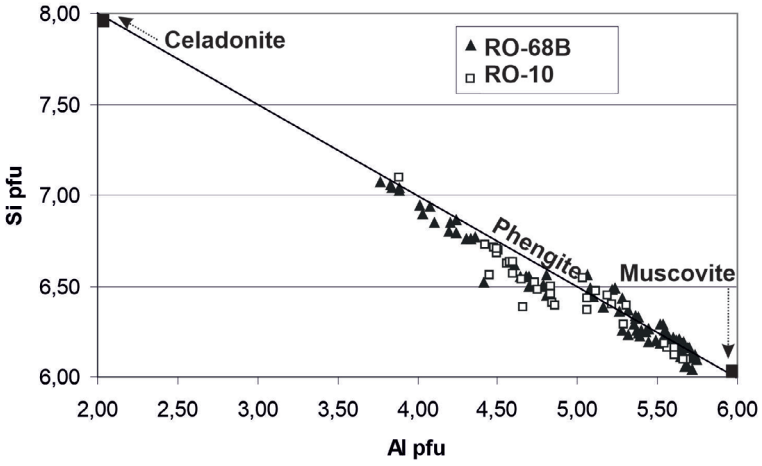

Fig. 4. Graphic representation of white mica composition of two dated samples in a diagram Al vs. Si per formula unit (pfu).

By contrast, sample RO-10 from the Late Cretaceous Rusca Montană basin of the South Carpathians (Fig. 1b for location) comprises dominantly Variscan and a few Triassic detrital mica grains, consistent with Variscan (309 to 301 Ma) and subordinate Triassic (>200 Ma) white mica ages of the underlying basement exposed in the Supra-Getic/Getic nappes (Dallmeyer et al. 1998a; Iancu et al. 2005). The Variscan white mica likely include also such with a considerable phengite content as the microprobe study testifies (Fig. 4), and similar phengite contents were reported by Săbău & Massonne (2003). The Danubian nappe complex with its dominant Cretaceous-aged greenschist facies overprint is exposed in the footwall of the Supragetic/Getic nappes and southerly adjacent to the Rusca Montană basin. Our new Ar–Ar ages from detrital white mica from the Rusca Montană basin, therefore, suggest that

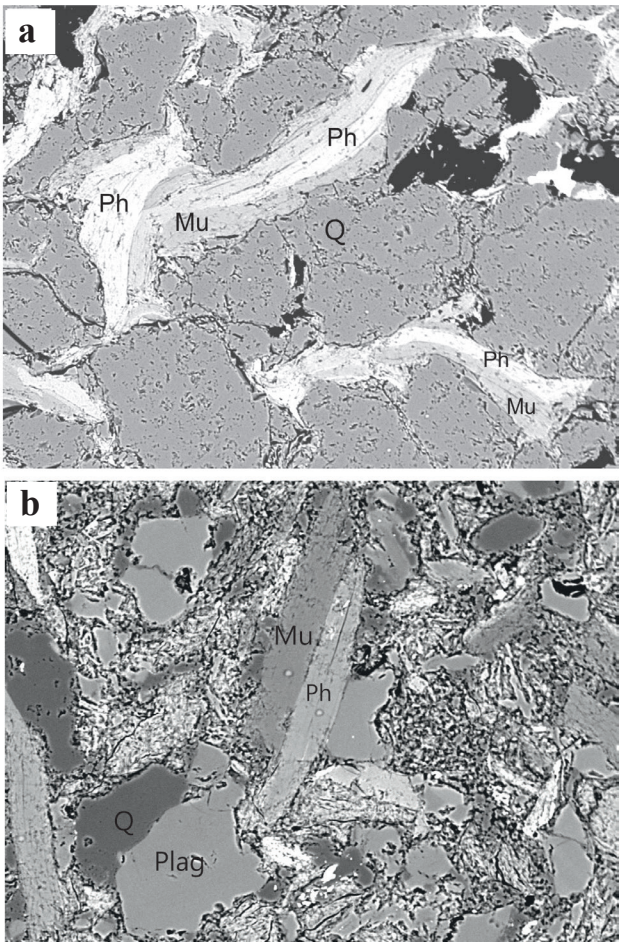

Fig. 5. Back-scattered image showing intergrowth of phengitic white mica with muscovite. **a** — Sample RO-68A, **b** — sample RO-10. Abbreviations: Ms – muscovite, Ph – phengite, Plag – plagioclase, Q – quartz.

the Danubian window was likely not exposed at the surface during the early Late Cretaceous as already Berza (2004) postulated from the analysis of granitic clasts. A source within the Getic nappe complex, which also formed the hangingwall above the exhuming Retezeat metamorphic dome, may represent the most likely source. Note, that similar Permian to Cretaceous-aged detrital white mica were found in the syn-orogenic Sinaia flysch deposits of the Danubian cover and Severin nappe (Neubauer & Bojar 2013).

The characteristically high proportion of young, Cretaceous detrital white micas in the Gosau-type Vlădeasa basin is a stark contrast to the Himalayan and Alpine molasse deposits in which the proportion of new micas comprises 20–30 percent (Copeland & Harrison 1990; Najman et al. 1997; von Eynatten et al. 1999; Carrapa et al. 2003; von Eynatten & Wijbrans 2003). This difference suggests an extreme denudation of the Variscan orogen down to levels of the argon retention temperature of white mica (~375–410 °C: McDougall & Harrison 1999; Villa 1998 and references therein and 425±25 °C according to Harrison et al. 2009) prior to molasse deposition. A normal thermal gradient of ~30 °C/km suggests denudation of ~12.5–14 km of crust.

The studied micas from the Vlădeasa basin Maastrichtian sandstone comprise a dominant Cretaceous-aged group and argue for the erosion of a medium-grade pressure-dominated metamorphic unit, which is not exposed in the surroundings of the present-day Apuseni Mts. except in the eastern part of the Baia de Aries nappe. The high proportion of phengitic white mica (Figs. 4, 5) argue for relatively high pressure of this unit. Consequently, the Apuseni Mts. must have been disrupted from such a source area and shifted along major strike-slip faults after the formation of the Vlădeasa basin. The question now arises, from which area the Apuseni-South Carpathian orogen invaded into the Carpathian arc. Previous models indicate that this orogen, including the magmatic Banatite belt of

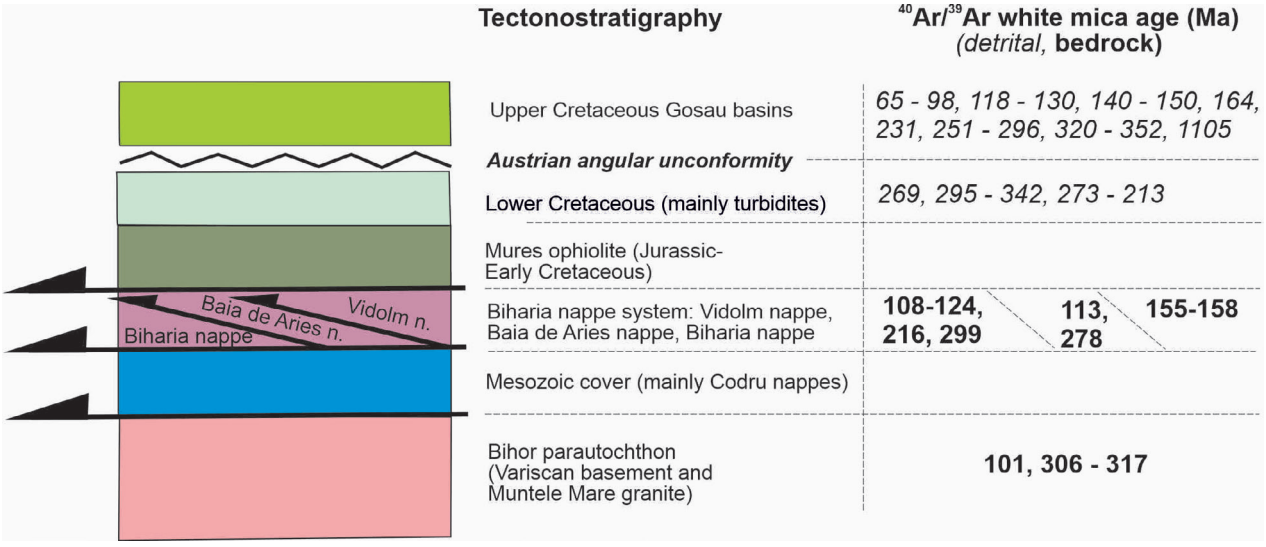

Fig. 6. Tectonostratigraphy of tectonic units in Apuseni Mts. with white mica $^{40}Ar/^{39}Ar$ ages of bed rocks and detrital $^{40}Ar/^{39}Ar$ ages.

Late Cretaceous age, formed an E–W stretching belt along the southern margin of the Moesian platform (e.g., Berza et al. 1998; Schmid et al. 1998; Neugebauer et al. 2001; Neubauer 2002; Stampfli et al. 2002; Fügenschuh & Schmid 2005; Gallhofer et al. 2015; van Hinsbergen et al. 2020), which was then clockwise rotated around the western Moesian platform (Márton et al. 2024; van Hinsbergen et al. 2020). Panafrican/Cadomian terranes were then exposed both in the north and south. The open question is the source of the early Variscan age group, which was rather widespread along the southern margins of the European plate and in the future Eastern Carpathians (Dallmeyer et al. 2000; Culshaw et al. 2012). A corresponding model showing possible linkages is shown in Fig. 7 and is based on the reconstruction proposed by Neugebauer et al. (2001), Neubauer (2002), von Quadt et al. (2005) and Schmid et al. (2008). The basic difference to the reconstruction of Neugebauer et al. (2001), Schmid et al. (2008) and Handy et al. (2010) is the displacement of 400 km of the Adriatic microplate back to the east to restore the 400 km Cenozoic dextral displacement along the ca. E–W striking Periadriatic fault. In that reconstruction, the area with pervasive Cretaceous metamorphic overprint in amphibolite facies metamorphic overprint, which is exposed to the west of the Apuseni Mts. (TD in Fig. 7), clearly demonstrates source linkages to Gosau basins of the Apuseni Mts.

Conclusions

The study of detrital white mica $^{40}Ar/^{39}Ar$ ages from Lower vs. Upper Cretaceous sandstones from Apuseni Mts. and South Carpathians allow the following major conclusions:

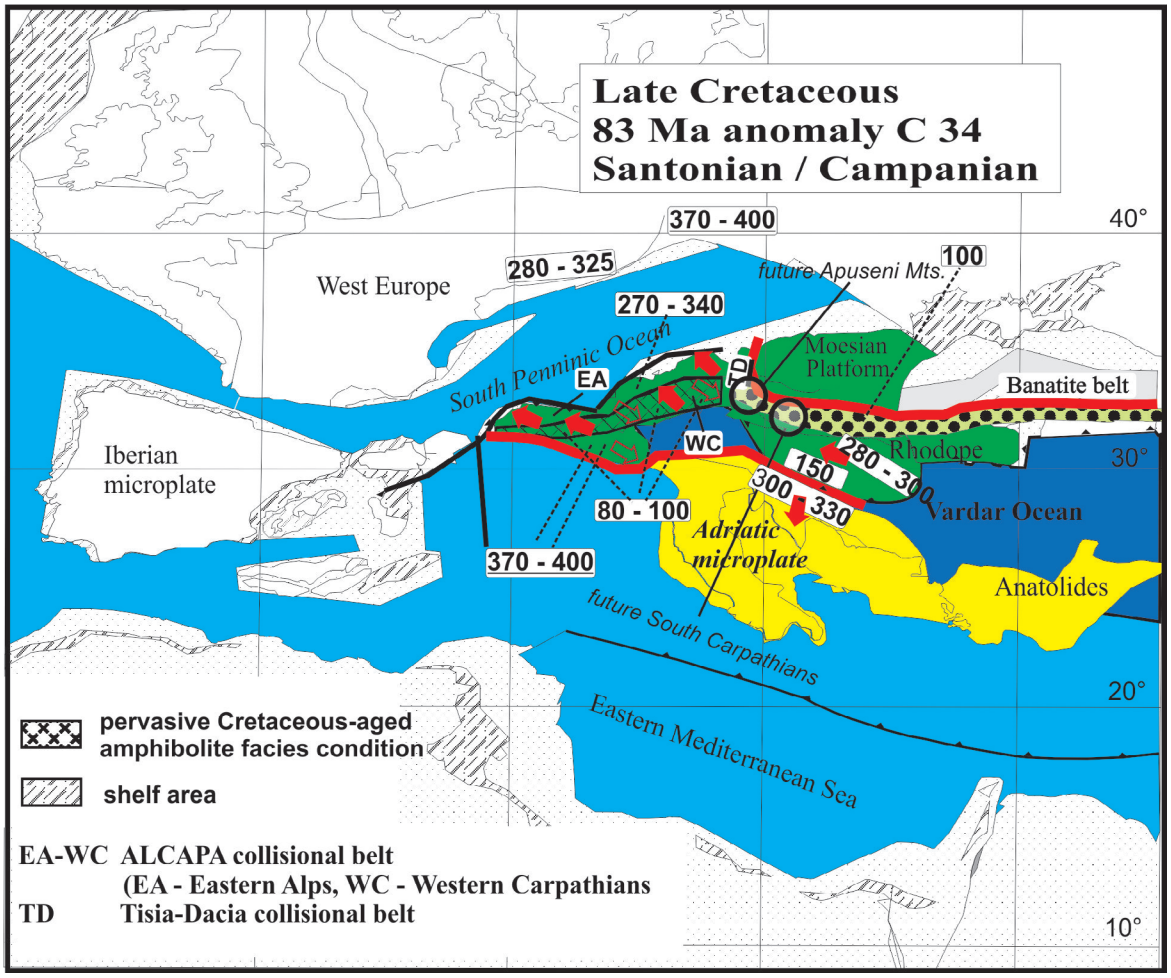

Fig. 7. Possible Santonian paleogeography of the Cretaceous-aged Alpine orogen stretching from the Alps through the Apuseni Mts. to the South Carpathians and the Srednogorie zone (modified after Neugebauer et al. 2001 and Neubauer 2002). Thick arrows show direction of Cretaceous thrust motion, open arrows of subsequent Late Cretaceous extension. The red lines represent the boundaries of the Cretaceous-aged Alpine orogen. The apparent displacement is sinistral to remove the future, Cenozoic offset of the dextral motion. The stable Adriatic plate is shifted ca. 450 km to the east compared to the amphibolite-grade ALCAPA units according to the Late Permian to Late Triassic facies reconstructions (Haas et al. 1995). Numbers indicate $^{40}Ar/^{39}Ar$ white mica ages in basement rocks and Carboniferous flysch (underlined). Data sources: Culshaw et al. 2012; Dallmeyer et al. 1996, 1998a, b, 1999, 2000; Gemignani et al. 2017; Ilic et al 2005; Lelkes-Felvári et al. 2003; Mader et al. 2007; Neubauer et al. 2007; Putiš et al. 2009; Vozárová et al. 2005.

- The Lower Cretaceous synorogenic flysch of Apuseni Mts. preserved memory on Early and Late Variscan orogenic metamorphic crust in the source region.
- The Late Cretaceous Gosau-type Vlădeasa collapse basin contains only a low percentage of Variscan micas and argue for the erosion of a medium-grade early Alpine metamorphic unit disrupted from the source area, which is potentially exposed subsurface in the southeastern Pannonian basin.
- In contrast, the Late Cretaceous Rusca Montană basin of South Carpathians comprises dominantly Variscan, only a few Triassic and no Cretaceous detrital mica grains. These are derived from the underlying Supra-Getic/Getic nappes.
- Consequently, Apuseni Mts. and South Carpathians reflect distinct sources for the Goau-type basins.

Acknowledgements: We gratefully acknowledge help by Tudor Berza, who advised field work and selected locations for sampling, and Robert Handler for handling samples. We gratefully acknowledge constructive suggestions by Dušan Plašienka, an anonymous reviewer, the latter with a characteristic review style, and by the associate editor. This work was supported by grant P15646-GEO of the Austrian Science Fund FWF to FN. Isabella Merschdorf corrected the English of the initial manuscript version.

References

Balintoni I., Balica C., Ducea M.N., Zaharia L., Chen F., Cliveți M., Hann H.P., Li L.-Q. & Ghergari L. 2010: Late Cambrian–Ordovician northeastern Gondwanan terranes in the basement of the Apuseni Mountains, Romania. *Journal of the Geological Society* 167, 1131–1145. https://doi.org/10.1144/0016-76492009-156

Barzoi S.C. & Seclaman M. 2010: Petrographic and geochemical interpretation of the Late Cretaceous volcaniclastic deposits from the Hateg Basin. *Palaeogeography, Palaeoclimatology, Palaeoecology* 293, 306–318. https://doi.org/10.1016/j.palaeo.2009.08.028

Berza T. 2004: Granitic pebbles in Upper Cretaceous red conglomerates of the Hateg Basin (Southern Carpathians, Romania): Geochemistry and provenance as clues in a tectonic controversy. *Geologica Carpathica* 55, 389–395.

Berza T., Constantinescu E. & Vlad S.N. 1998: Upper Cretaceous Magmatic Series and Associated mineralisation in the Carpathian–Balkan Orogen. *Resource Geology* 48:291–306.

Bojar A.V., Bojar H.P., Ottner F. & Grigorescu D. 2010: Heavy mineral distributions of Maastrichtian deposits from the Haţeg basin, South Carpathians: Tectonic and palaeogeographic implications. *Palaeogeography, Palaeoclimatology, Palaeoecology* 293, 319–328. https://doi.org/10.1016/j.palaeo.2009.10.002

Bordea S. 1971: Date stratigrafice și tectonice noi în zona Blăjeni – Buceș Vulcan (Munții Metaliferi). *Dări De Seamă Inst. Geol.* LVII/4,17–26.

Bordea S. & Constantinescu R. 1975: Blăjeni sheet of the 1:50.000 scale geological map of Romania. *Geological Institute of Romania*, Bucharest.

Carrapa B., Wijbrans J. & Bertotti G. 2003: Episodic exhumation in the Western Alps. *Geology* 31, 601–604. https://doi.org/10.1130/0091-7613(2003)031%3C0601:EEITWA%3E2.0.CO;2

Ciulavu M., Ferreiro-Mahlmann R., Seghedi A. & Frey M. 2001: Very low-grade metamorphism in the Danubian window, South Carpathians (Romania). *Terra Abstracts EUG* 11, 230–231.

Copeland P. & Harrison T.M. 1990: Episodic uplift in the Himalaya revealed by $^{40}Ar/^{39}Ar$ analysis of detrital feldspar and muscovite, Bengal fan. *Geology* 18, 354–357. https://doi.org/10.1130/0091-7613(1990)018%3C0354:ERUITH%3E2.3.CO;2

Culshaw N., Mosonyi E. & Reynolds P. 2012: New $^{40}Ar/^{39}Ar$ laser single-grain ages of muscovites from mylonitic schists in the Rodna Mountains, Eastern Carpathians, Romania: correlations with microstructure. *International Journal of Earth Sciences (Geologische Rundschau)* 101, 291–306. https://doi.org/10.1007/s00531-011-0674-y

Dachs E. 2004: PET: Petrological Elementary Tools for Mathematica (R): an update. *Computers & Geosciences* 30, 173–182. https://doi.org/10.1016/j.cageo.2003.09.007

Dallmeyer R.D., Neubauer F., Handler R., Fritz H., Müller W., Pană D. & Putiš M. 1996: Tectonothermal evolution of the internal Alps and Carpathians: Evidence from $^{40}Ar/^{39}Ar$ mineral and whole rock data. *Eclogae Geologicae Helvetiae* 89, 203–227.

Dallmeyer R.D., Neubauer F., Fritz H. & Mocanu V. 1998a: Variscan vs. Alpine tectonothermal evolution of the South Carpathian orogen: constraints from $^{40}Ar/^{39}Ar$ ages. *Tectonophysics* 290, 111–135. https://doi.org/10.1016/S0040-1951(98)00006-7

Dallmeyer R.D., Handler R., Neubauer F. & Fritz H. 1998b: Sequence of thrusting within a thick-skinned tectonic wedge. Evidence from $^{40}Ar/^{39}Ar$ ages from the Austroalpine nappe complex of the Eastern Alps. *Journal of Geology* 106, 71–86. https://doi.org/10.1086/516008

Dallmeyer R.D., Pană D., Neubauer F. & Erdmer P. 1999: Tectonothermal evolution of the Apuseni mountains. Romania: resolution of Variscan versus Alpine events with $^{40}Ar/^{39}Ar$ ages. *Journal of Geology* 107, 329–352. https://doi.org/10.1086/314352

Dallmeyer R.D., Neubauer F., Kräutner H.G. & Bojar A.-V. 2000: Variscan and Alpine tectonic processes in the pre-Alpine basement of the Eastern Carpathian orogen: Evidence from $^{40}Ar/^{39}Ar$ mineral ages and structural analysis. In: *15th International Conference on Basement Tectonics, Santiago de Compostela, Abstract Volume*, 113.

Ducea M.N., Giosan L., Carter A., Balica C., Stoica A.M., Roban R.D., Balintoni I., Filip F. & Petrescu L. 2018: U–Pb detrital zircon geochronology of the lower Danube and its tributaries: Implications for the geology of the Carpathians. *Geochemistry, Geophysics, Geosystems* 19, 3208–3223. https://doi.org/10.1029/2018GC007659

Fügenschuh B. & Schmid S.M. 2005: Age and significance of core complex formation in a very curved orogen: Evidence from fission track studies in the South Carpathians (Romania). *Tectonophysics* 404, 33–53. https://doi.org/10.1016/j.tecto.2005.03.019

Gallhofer D., von Quadt A., Peytcheva I., Schmid S.M. & Heinrich C.A. 2015: Tectonic, magmatic, and metallogenic evolution of the Late Cretaceous arc in the Carpathian-Balkan orogen. *Tectonics* 34, 1813–1836. https://doi.org/10.1002/2015TC003834

Gallhofer D., von Quadt A., Schmid S.M., Guillong M., Peytcheva I. & Seghedi I. 2017: Magmatic and tectonic history of Jurassic ophiolites and associated granitoids from the South Apuseni Mountains (Romania). *Swiss Journal of Geosciences* 110, 699–719. https://doi.org/10.1007/s00015-016-0231-6

Gemignani L., Sun X., Braun J., van Gerve T.D. & Wijbrans J.R. 2017: A new detrital mica $^{40}Ar/^{39}Ar$ dating approach for provenance and exhumation of the Eastern Alps. *Tectonics* 36, 1521–1537. https://doi.org/10.1002/2017TC004483

Haas J., Kovács S., Krystyn L. & Lein R. 1995: Significance of Late Permian–Triassic facies zones in terrane reconstructions in the Alpine–North Pannonian domain. *Tectonophysics* 242, 19–40.

Handler R., Dallmeyer R.D. & Neubauer F. 1997: $^{40}Ar/^{39}Ar$ ages of detrital white mica from Austroalpine units in the Eastern Alps, Austria: Evidence for Cadomian and contrasting Variscan sources. *Geologische Rundschau* 86, 69–80.

Handler R., Velichkova S.H., Neubauer F. & Ivanov Z. 2004: $^{40}Ar/^{39}Ar$ age constraints on the timing of magmatism and post-magmatic cooling in the Panagyurishte region, Bulgaria. *Schweizerische Mineralogische und Petrographische Mitteilungen* 84, 119–132.

Handy M.R., Schmid S.M., Bousquet R., Kissling E. & Bernoulli D. 2010: Reconciling plate-tectonic reconstructions of Alpine Tethys with the geological-geophysical record of spreading and subduction in the Alps. *Earth-Science Reviews* 102, 121–158. https://doi.org/10.1016/j.earscirev.2010.06.002

Harrison T.M., Célérier J., Aikman A.B., Hermann J. & Heizler M.T. 2009: Diffusion of ^{40}Ar in muscovite. *Geochimica et Cosmochimica Acta* 73, 1039–1051. https://doi.org/10.1016/j.gca.2008.09.038

Hodges K.V., Ruhl K.W., Wobus C.W. & Pringle M.S. 2005: $^{40}Ar/^{39}Ar$ Thermochronology of Detrital Minerals. *Reviews of Mineralogy and Geochemistry* 58, 239–257. https://doi.org/10.2138/rmg.2005.58.9

Hoinkes G., Koller F., Rantitsch G., Dachs E., Höck V., Neubauer F. & Schuster R. 1999: Alpine metamorphism in the Eastern Alps. *Schweizerische Mineralogisch-Petrographische Mitteilungen* 79, 155–181.

Iancu V., Berza T., Seghedi A., Gheuca I. & Hann H.P. 2005: Alpine polyphase tectono-metamorphic evolution of the South Carpathians: A new overview. *Tectonophysics* 410, 337–365. https://doi.org/10.1016/j.tecto.2004.12.038

Ilic A., Neubauer F. & Handler R. 2005: Late Paleozoic-Mesozoic tectonics of Dinarides revisited: implications from $^{40}Ar/^{39}Ar$ dating of detrital white micas. *Geology* 33, 233–236. https://doi.org/10.1130/G20979.1

Kondor H. & Tóth T.M. 2025: Metamorphic and post-metamorphic evolution of the SE part of the Pannonian Basin in the Algyő–Ferencszállás crystalline high: Thermobarometric constraints on Variscan to Alpine events. *Geologica Carpathica* 76, 71–91. https://doi.org/10.31577/GeolCarp.2025.09

Kounov A. & Schmid S.M. 2012: Fission-track constraints on the thermal and tectonic evolution of the Apuseni Mountains (Romania). *International Journal of Earth Sciences (Geologische Rundschau)* 102, 207–233. https://doi.org/10.1007/s00531-012-0800-5

Lelkes-Felvári G., Frank W. & Schuster R. 2003: Geochronological constraints of the Variscan, Permian-Triassic and eo-Alpine (Cretaceous) evolution of the Great Hungarian Plain basement. *Geologica Carpathica* 54, 299–315.

Lelkes-Felvári G., Schuster R., Frank W. & Sassi R. 2005: Metamorphic history of the Algyő High (Tisza Mega-unit, basement of Great Hungarian Plain) – a counterpart of crystalline units of the Koralpe-Wölz nappe system (Austroalpine, Eastern Alps). *Acta Geologica Hungarica* 48, 371–394. https://doi.org/10.1556/ageol.48.2005.4.2

Liégeois J.P., Berza T., Tatu M. & Duchesne J.C. 1996: The Neoproterozoic Pan-African basement from the Alpine Lower Danubian nappe system (South Carpathians, Romania). *Precambrian Research* 80, 281–301.

Ludwig K.R. 2005: Isoplot/Ex - A Geochronological Toolkit for Microsoft Excel. Berkeley Geochronological Center Special Publication No. 1a. http://www.bgca.org/klprogrammenu.html

Mader D., Neubauer F. & Handler R. 2007: $^{40}Ar/^{39}Ar$ dating of detrital white mica of Late Palaeozoic sandstones in the Carnic Alps (Austria): implications to provenance and tectonic setting of sedimentary basins. *Geologica Carpathica* 58, 133–144.

Márton E., Cvetkov E., Banješević M., Imre G. & Pačevski A. 2024: Tectonic evolution of the Circum-Moesian orocline of the Carpatho-Balkanides: Paleomagnetic constraints. *Journal of Geodynamics* 162, 102058. https://doi.org/10.1016/j.jog.2024.102058

McDougall I. & Harrison M.T. 1999: Geochronology and thermochronology by the $^{40}Ar/^{39}Ar$ method (2nd Ed.) *Oxford University Press*, Oxford, 1–269.

Medaris J.G., Ducea M.N., Ghent E. & Iancu V. 2003: Conditions and timing of high-pressure Variscan meta-morphism in the South Carpathians, Romania. *Lithos* 70, 141–161. https://doi.org/10.1016/S0024-4937(03)00096-3

Melinte-Dobrinescu M.C. 2010: Lithology and biostratigraphy of Upper Cretaceous marine deposits from the Haţeg region (Romania): Palaeoenvironmental implications. *Palaeogeography, Palaeoclimatology, Palaeoecology* 293, 283–294. https://doi.org/10.1016/j.palaeo.2009.04.001

Merten S., Matenco L., Foeken J.P.T. & Andriessen P.A.M. 2011: Toward understanding the post-collisional evolution of an orogeny influenced by convergence at adjacent plate margins: Late Cretaceous–Tertiary thermotectonic history of the Apuseni Mountains. *Tectonics* 30, TC6008. https://doi.org/10.1029/2011TC002887

Najman Y.M.R., Pringle M.S., Johnson M.R.W., Robertson A.H.F. & Wijbrans J.R. 1997: Laser $^{40}Ar/^{39}Ar$ dating of single detrital muscovite grains from early foreland-basin sedimentary deposits in India: Implications for early Himalayan evolution. *Geology* 25, 535–538.

Neubauer F. 2002: Contrasting Late Cretaceous to Neogene ore provinces in the Alpine-Balkan-Carpathian-Dinaride collision belt. In: Blundell D.J., Neubauer F. & Quadt A. (Eds): The timing and location of major ore deposits in an evolving orogen. *Geological Society (London) Special Publication* 204, 81–102. https://doi.org/10.1144/GSL.SP.2002.204.01.06

Neubauer F. & Bojar A.V. 2013: Origin of sediments during Cretaceous continent-continent collision in the Romanian South Carpathians: preliminary constraints from $^{40}Ar/^{39}Ar$ single-grain dating of detrital white mica. *Geologica Carpathica* 56, 375–382. https://doi.org/10.2478/geoca-2013-0025

Neubauer F., Friedl G., Genser J., Handler R., Mader D. & Schneider D. 2007: Origin and tectonic evolution of Eastern Alps deduced from dating of detrital white mica: a review. *Austrian Journal of Earth Sciences* 100, 8–23.

Neubauer F., Chang R.-H., Dong Y.-P., Genser J. & Liu Y.-J. 2025: Unravelling the history of mountain belts through U–Pb and Lu–Hf dating of zircon and $^{40}Ar/^{39}Ar$ dating of detrital white mica: a case study from the Eastern Alps. *Isotopes in Environmental and Health Studies* 61, 114–132. https://doi.org/10.1080/10256016.2024.2367099

Neugebauer J., Greiner B. & Appel E. 2001: Kinematics of Alpine–West Carpathian orogen and palaeogeographic implications. *Journal of the Geological Society (London)* 158, 97–110. https://doi.org/10.1144/jgs.158.1.97

Obbágy G., Dunkl I., Józsa S., Silye L., Arató R., Lünsdorf N.K. & von Eynatten H. 2021: Paleogeographic implications of a multi-parameter Paleogene provenance dataset (Transylvanian basin, Romania). *Journal of Sedimentary Research* 91, 551–570. https://doi.org/10.2110/jsr.2020.080

Pană D.I., Heaman L.M., Creaser R.A. & Erdmer P. 2002: Pre-Alpine crust in the Apuseni Mountains, Romania; insights from Sm–Nd and U–Pb data. *Journal of Geology* 110, 341–354. https://doi.org/10.1086/339536

Putiš M., Frank W., Plašienka D., Siman P., Sulák M. & Biroň A. 2009: Progradation of the Alpidic Central Western Carpathians orogenic wedge related to two subductions: Constrained by $^{40}Ar/^{39}Ar$ ages of white micas. *Geodinamica Acta* 22, 31–56. https://doi.org/10.3166/ga.22.31-56

Ratschbacher L., Linzer G.H., Moser F., Strusievicz R.O., Bedelean H., Har N. & Mogos P.A. 1993: Cretaceous to Miocene thrusting and wrenching along the central South Carpathians due to a corner effect during collision and orocline formation. *Tectonics* 12, 855–873.

Reiser M.K., Schuster R., Spikings R., Tropper P. & Fügenschuh B. 2017: From nappe stacking to exhumation: Cretaceous tectonics in the Apuseni Mountains (Romania). *International Journal of Earth Sciences (Geologische Rundschau)* 106, 659–685. https://doi.org/10.1007/s00531-016-1335-y

Săbău G. & Massonne H.-J. 2003. Relationships Among Eclogite Bodies and Host Rocks in the Lotru Metamorphic Suite (South Carpathians, Romania): Petrological Evidence for Multistage Tectonic Emplacement of Eclogites in a Medium-Pressure Terrain. *International Geology Review* 45, 225–262. https://doi.org/10.2747/0020-6814.45.3.225

Sandulescu M. 1984: Geotectonica Romaniei. *Editura Tehnica*, Bucharest, 1–336.

Schmid S.M., Berza T., Diaconescu V., Froitzheim N. & Fügenschuh B. 1998: Orogen-parallel extension in the Southern Carpathians. *Tectonophysics* 297, 209–228.

Schmid S.M., Bernoulli D., Fügenschuh B., Matenco L., Schefer S., Schuster R., Tischler M. & Ustaszewski K. 2008: The Alpine–Carpathian–Dinaridic orogenic system: correlation and evolution of tectonic units. *Swiss Journal of Geosciences* 101, 139–183. https://doi.org/10.1007/s00015-008-1247-3

Schneider D. 2002: $^{40}Ar/^{39}Ar$ dating of detrital white mica, geochemistry and detrital mode of peripheral foreland basins (Molasse and Silesian basins). *PhD thesis, University of Salzburg*, 1–184.

Schuller V. 2004: Evolution and geodynamic significance of the Upper Cretaceous Gosau basin in the Apuseni Mountains (Romania). *Tübinger Geowissenschaftliche Arbeiten* A70, 1–112.

Schuller V. & Frisch W. 2006: Heavy mineral provenance and paleocurrent data of the Upper Cretaceous Gosau succession of the Apuseni Mountains (Romania). *Geologica Carpathica* 57, 29–39.

Schuller V., Frisch W., Danišík M., Dunkl I. & Melinte M.C. 2009: Upper Cretaceous Gosau deposits of the Apuseni Mountains (Romania) – similarities and differences to the Eastern Alps. *Austrian Journal of Earth Sciences* 102, 133–145.

Sircombe K.N. 2004: AgeDisplay; an EXCEL workbook to evaluate and display univariate geochronological data using binned frequency histograms and probability density distributions. *Computers & Geosciences* 30, 21–31.

Stampfli G.M., Borel G.D., Marchant R. & Mosar J. 2002: Western Alps geological constraints on western Tethyan reconstructions. *Journal of Virtual Explorer* 8, 77–106. https://doi.org/10.1016/j.cageo.2003.09.006

Steiger R.H. & Jäger E. 1977: Subcommission on geochronology: Convention on the use of decay constants in geo-and cosmochronology. *Earth and Planetary Science Letters* 36, 359–362.

Therrien F. 2005: Palaeoenvironments of the latest Cretaceous (Maastrichtian) dinosaurs of Romania: insights from fluvial deposits and paleosols of the latest Cretaceous (Maastrichtian) dinosaurs of Romania: insights from fluvial deposits and paleosols of the Transylvanian and Haţeg basins. *Palaeogeography, Palaeoclimatology, Palaeoecology* 218, 15–56. https://doi.org/10.1016/j.palaeo.2004.12.005

Therrien F. 2006: Depositional environments and fluvial system changes in the dinosaur-bearing Sanpetru Formation (Late Cretaceous, Romania): Post-orogenic sedimentation in an active extensional basin. *Sedimentary Geology* 192, 183–205. https://doi.org/10.1016/j.sedgeo.2006.04.002

Vander Auwera J., Berza T., Gesels J. & Dupont A. 2016: The Late Cretaceous igneous rocks of Romania (Apuseni Mountains and Banat): The possible role of amphibole versus plagioclase deep fractionation in two different crustal terranes. *International Journal of Earth Sciences* 105, 819–847. https://doi.org/10.1007/s00531-015-1210-2

van Hinsbergen D.J.J., Torsvik T.H., Schmid S.,Matenco L.C., Maffione M., Vissers R.L.M., Gürer D. & Spakman W. 2020: Orogenic architecture of the Mediterranean region and kinematic reconstruction of its tectonic evolution since the Triassic. *Gondwana Research* 81, 79–229. https://doi.org/10.1016/j.gr.2019.07.009

Van Itterbeeck J., Sasaran E. & Codrea V. 2004: Sedimentology of the Upper Cretaceous mammal- and dinosaur-bearing sites along the Raul Mare and Barbat Rivers, Hateg Basin, Romania. *Cretaceous Research* 25, 517–530. https://doi.org/10.1016/j.cretres.2004.04.004

Villa I. 1998: Isotopic closure. *Terra Nova* 10, 42–47. https://doi.org/10.1046/j.1365-3121.1998.00156.x

von Eynatten H. & Wijbrans J.R. 2003: Precise tracing of exhumation and provenance using $^{40}Ar/^{39}Ar$ geochronology of detrital white mica: the example of the Central Alps. In: McCann T. & Saintot A. (Eds.): Tracing tectonic deformation using the sedimentary record. *Geological Society (London) Special Publication* 208, 289–305. https://doi.org/10.1144/GSL.SP.2003.208.01.14

von Eynatten H., Gaupp R., Wijbrans J.R. 1996: $^{40}Ar/^{39}Ar$ laser-probe dating of detrital white micas from Cretaceous sedimentary rocks of the Eastern Alps: Evidence for Variscan high-pressure metamorphism and implications for Alpine orogeny. *Geology* 24, 691–694. https://doi.org/10.1130/0091-7613(1996)024%3C0691:AALPDO%3E2.3.CO;2

von Eynatten H., Schlunegger F., Gaupp R. & Wijbrans J.R. 1999: Exhumation of the Central Alps: Evidence from $^{40}Ar/^{39}Ar$ laser-probe dating of detrital white micas from the Swiss Molasse Basin. *Terra Nova* 11, 284–289. https://doi.org/10.1046/j.1365-3121.1999.00260.x

von Quadt A., Moritz R., Peytcheva I. & Heinrich C.A. 2005: Geochronology and Geodynamics of Late Cretaceous magmatism and Cu-Au mineralization in the Panagyurishte region of the Apuseni-Banat-Timok-Srednogorie belt, Bulgaria. *Ore Geology Reviews* 27, 95–126. https://doi.org/10.1016/j.oregeorev.2005.07.024

Vornicu V.M., Seghedi I., Csiki-Sava Z. & Ducea M.N. 2023: Campanian U–Pb ages of volcaniclastic deposits of the Haţeg Basin (Southern Carpathians): Implications for future intrabasinal lithostratigraphic correlations. *Geologica Carpathica* 74, 407–422. https://doi.org/10.31577/GeolCarp.2023.21

Vozárová A., Frank W., Kráľ J. & Vozár J. 2005: $^{40}Ar/^{39}Ar$ dating of detrital mica from the Upper Paleozoic sandstones in the Western Carpathians (Slovakia). *Geologica Carpathica* 56, 463–472.

Wagreich M. & Faupl P. 1994: Palaeogeography and geodynamic evolution of the Gosau Group of the Northern Calcareous Alps (Late Cretaceous, Eastern Alps, Austria). *Palaeogeography, Palaeoclimatology, Palaeoecology* 110, 235–254.

Wijbrans J.R., Pringle M.S., Koopers A.A.P. & Schveers R. 1995: Argon geochronology of small samples using the Vulkaan argon laserprobe. *Proc. Koninklijke Academie Wetenschappen* 98, 185–218.

Willingshofer W., Neubauer F. & Cloetingh S. 1999: Significance of Gosau basins for the Upper Cretaceous geodynamic history of the Alpine-Carpathian belt. *Physics and Chemistry of the Earth* 24, 687–695. https://doi.org/10.1016/S1464-1895(99)00100-3

Willingshofer E., Andriessen P., Cloetingh S. & Neubauer F. 2001: Detrital fission track thermochronology of Upper Cretaceous synorogenic sediments in the South Carpathians (Romania); inferences on the tectonic evolution of a collisional hinterland. *Basin Research* 13, 379–395. https://doi.org/10.1046/j.0950-091x.2001.00156.x

Appendix 1: Sample locations and description

Sample RO-33

Location: N 46°13'14.6", E 22°57'49.7", Map sheet 73b Blajeni (1:50 000). Samples are taken on the road no. 74, from Brad to Abrud. Sampled in the first, strongly to the left bending curve, about 1 km before the village Buces Vulcan. Aptian to Hauterivian "Shaley Flysch" (sandstones, shales and marls) according to Bordea & Constantinescu (1975).

Sample RO-34

Location: N 46°13'14.6", E 22°57'49.7" Map sheet 73b Blajeni (1:50 000). Sample was taken about 1 km south of sample RO-33 in the Buces valley. Maastrichtian detrital series "Mica-Flysch". It represents a sandy to calcareous, sometimes coarse-grained sandstone according to Bordea & Constantinescu (1975).

Sample RO-68B

Location: N 46°48'56.6", E 22°35'12.1". Vlădeasa basin of North Apuseni Mts. Sample was taken in the Upper Cretaceous Gosau Group from a road cut in the Iad valley close to the power station dam of the Iad river. Map sheet 41c Stana de Vale (1:50 000) was not printed yet at the time of sampling.

Sample RO-10

Location: Pleschu valley, ca. 2.6 km NW Gura tributary, Valea Negri. Sample was taken in the Upper Cretaceous Gosau Formation of the Rusca Montană Mts., north-western South Carpathians. Map sheet 105b (1:50 000) Hateg. No GPS coordinates are available for this sample.

Appendix 2: $^{40}Ar/^{39}Ar$ analytical techniques

Preparation of the samples before and after irradiation, $^{40}Ar/^{39}Ar$ analyses, and age calculations were carried out at the ARGONAUT Laboratory of the Dept. of Environment and Biodiversity at the Paris-Lodron-University of Salzburg, Austria. Mineral concentrates are packed in aluminum-foil and loaded in quartz vials. For calculation of the J-values, flux-monitors are placed between each 4–5 unknown samples, which yield a distance of ca. 5 mm between adjacent flux-monitors. The sealed quartz vials are irradiated in the MTA KFKI reactor (Debrecen, Hungary) for 16 hours. Correction factors for interfering isotopes were calculated from 10 analyses of two Ca-glass samples and 22 analyses of two pure K-glass samples, and are: $^{36}Ar/^{37}Ar_{(Ca)}=0.00026025$, $^{39}Ar/^{37}Ar_{(Ca)}=0.00065014$, and $^{40}Ar/^{39}Ar_{(K)}=0.015466$. Variation in the flux of neutrons were monitored with DRA1 sanidine standard for which a $^{40}Ar/^{39}Ar$ plateau age of 25.03±0.05 Ma has been reported (Wijbrans et al. 1995). After irradiation the minerals are unpacked from the quartz vials and the aluminum-foil packets, and hand-picked into 1 mm diameter holes of the one-way Al-sample holders.

$^{40}Ar/^{39}Ar$ analyses are carried out using a UHV Ar-extraction line equipped with a combined MERCHANTEK™ UV/IR laser system, and a VG-ISOTECH™ NG3600 mass spectrometer. Stepwise heating analyses of samples are performed using a defocused (~1.5 mm diameter) 25 W CO_2-IR laser operating in Tem_{00} mode at wavelengths between 10.57 and 10.63 µm. The laser is controlled from a PC, and the position of the laser on the sample is monitored on the computer screen via a video camera in the optical axis of the laser beam through a double-vacuum window on the sample chamber. Gas clean-up is performed using one hot and one cold Zr–Al SAES getter. Gas admittance and pumping of the mass spectrometer and the Ar-extraction line are computer controlled using pneumatic valves. The NG3600 is a 18 cm radius 60° extended geometry instrument, equipped with a bright Nier-type source operated at 4.5 kV. Measurements are performed on an axial electron multiplier in static mode, peak-jumping and stability of the magnet is controlled by a Hall-probe. For each increment the intensities of ^{36}Ar, ^{37}Ar, ^{38}Ar, ^{39}Ar, and ^{40}Ar are measured, the baseline readings on mass 35.5 are automatically subtracted. Intensities of the peaks are back-extrapolated over 16 measured intensities to the time of gas admittance either by a straight line or a curved fit, depending on intensity and type of pattern of the evolving gas. Intensities are corrected for system blanks, background, post-irradiation decay of ^{37}Ar, and interfering isotopes. Isotopic ratios, ages and errors for individual steps are calculated following suggestions by McDougall & Harrison (1999) using decay factors reported by Steiger & Jäger (1977). Definition and calculation of plateau ages was carried out using ISOPLOT/EX (Ludwig 2005).

Appendix 3: Electron microprobe analytical technique

Polished thin sections of two samples were analyzed using a fully automated JEOL 8600 electron microprobe at the Geology Division of the University of Salzburg, Austria. Point analyses were obtained using a 15 kV accelerating voltage and 40 nA beam current. The beam size was set to 5 µm. Natural and synthetic oxides and silicates were used as standards for major elements. Structural formulas for white mica were calculated and plotted on the basis of 22 O using the Mathematica package based software PET (Dachs 2004).